Talanta 203 (2019) 9–15

Contents lists available at ScienceDirect

Talanta

journal homepage: www.elsevier.com/locate/talanta

A Surface Acoustic Wave (SAW) biosensor method for functional quantification of *E. coli* L-asparaginase

Han Yao, Cristina Soto Fernández, Xiaolong Xu, Evelien Wynendaele, Bart De Spiegeleer*

Drug Quality and Registration (DruQuaR) Group, Department of Pharmaceutical Analysis, Faculty of Pharmaceutical Sciences, Ghent University, Ottergemsesteenweg 460, 9000 Ghent, Belgium

ARTICLE INFO

Keywords:
Surface acoustic wave (SAW) biosensor
L-asparaginase
Method development and validation

ABSTRACT

Biosensors are rising technologies in the pharmaceutical field for medicine discovery, development and Quality Control (QC) stages. Surface acoustic wave (SAW) biosensor employs acoustic waves generated by oscillating a piezoelectric crystal quartz plate to meas. mass and viscosity, and allows to detect and quantify binding events between the analyte and an immobilized interacting ligand. We present here a SAW biosensor based approach for the functional quantification of *Escherichia coli* L-asparaginase (*E. coli* L-ASNase), using polyclonal antibody (pAb) as the interaction partner immobilized on the chip. Different immobilization strategies of pAb were initially evaluated, resulting in the BS^3 activated amide coupling via protein G strategy as the final immobilization method. The method was validated by evaluating the selectivity, linearity, as well as accuracy (a recovery of 102.4%) and precision (RSD of 8.5%). The application of the validated method on different samples encompassing different lots of *E. coli* L-ASNase, deamidated *E. coli* L-ASNase and dry-heated *E. coli* L-ASNase (80 °C, 10 min) indicated the suitability of the developed SAW method to quantify *E. coli* L-ASNase. We suggest this SAW method can be adopted as a pharmaceutical QC method.

1. Introduction

L-asparaginase (L-ASNase) is a tetrameric enzyme, and has been a universal component of therapy for pediatric acute lymphoblastic leukaemia (ALL) since 1970's [1]. The clinically used L-ASNase preparations are derived from *Escherichia coli* (*E. coli*) or from *Erwinia chrysanthemi* [1], with a tetrameric molecular weight (MW) of 136 320 Da resp. 140 320 Da [2,3]. The mechanism of anti-ALL activity of L-ASNase is that leukemic cells cannot synthesize themselves sufficient L-asparagine (L-Asn) required for their protein synthesis; leukemic cells therefore have to depend upon the external L-Asn supply from the plasma and tissues [4]. The administration of L-ASNase quenches the external source of L-Asn, hence starving cancer cells [4]. For the treatment of pediatric ALL, remission induction therapy including L-ASNase, vincristine, corticosteroid and anthracycline has been the mainstay of the initial stage of the treatment [5]. In the consolidation phase of treatment, L-ASNase is also adopted in the therapy together with methotrexate, 6-mercaptopurine, vincristine and/or prednisone [5]. Three forms of L-ASNase are currently used in clinical practice, namely: (native) *E. coli* L-ASNase, PEGylated *E. coli* L-ASNase, and *Erwinia* L-ASNase [5]. Among these forms, *E. coli* L-ASNases are used for first-line treatment of ALL, whereas *Erwinia* L-ASNase is used as second or third line treatment [6]. In this study, *E. coli* L-ASNase was investigated by a biosensor based functional quantification method, with an anti- *E. coli* L-ASNase antibody used as the analytical interaction partner.

Acoustic wave biosensors is a nanogram sensitive technology, employing acoustic waves generated by oscillating a piezoelectric crystal quartz plate to meas. mass and viscosity changes [7]. Acoustic wave biosensors can be classified into surface acoustic wave (SAW), bulk acoustic wave, and acoustic plate mode devices depending on the acoustic wave guiding process [8]. A surface acoustic wave is a mechanical acoustic wave that propagates to a confined area of a piezoelectric crystal [9]. Love wave SAW sensor is a recent developed device developed for integration in lab-on-a-chip systems. Love waves propagate near the surface of the piezoelectric material, the velocity and the amplitude of the wave depend on the changes occurring in the media near the surface [9]. The SAW biosensor proved to be a sensitive and effective technology for label-free detection of molecular interactions. Binding reactions are detected by measuring changes in surface wave velocity mainly caused by mass adsorption or viscosity changes on the surface layer [10]. Using SAW instruments as biosensors, antibodies or receptors are immobilized on the sensing layer to bind with analytes, using a hydrogel layer on the sensor surface [11]. To date, a wide range

* Corresponding author.
E-mail address: Bart.DeSpiegeleer@UGent.be (B. De Spiegeleer).

https://doi.org/10.1016/j.talanta.2019.05.046
Received 8 March 2019; Received in revised form 6 May 2019; Accepted 9 May 2019
Available online 11 May 2019

of analytes have been studied by SAW, involving proteins, DNA, large cells and bacteria [12–17], mostly from a diagnostic and therapeutic perspective [15,18,19].

Up till now, only a few biosensor approaches have recently been reported, using L-ASNase as immobilized ligand for the determination of other analytes [20–22]. A surface plasmon resonance (SPR) method for the rapid detection of anti-ASNase antibodies was developed, using L-ASNase as the binding target immobilized on the chip surface [21]. In another study, one microplate-based biosensor was used for the determination of the L-asparagine in biological samples, with the L-ASNase immobilized on the microplate, based on the colorimetric meas. ment of ammonia formation using the Nessler's reagent [22]. Until now, no SAW or other biosensor method has been reported for the determination of L-ASNase itself. In this study, we developed a SAW biosensor based functional quantification method for *E. coli* L-ASNase. The pAb of *E. coli* L-ASNase was immobilized on the chip, with *E. coli* L-ASNase as the running analyte. After an initial immobilization investigation, the method was validated and applied on different *E. coli* L-ASNase samples.

2. Materials and methods

2.1. Materials and equipment

Chemicals were purchased from Sigma-Aldrich (Diegem, Belgium) and Merck (Overijse, Belgium). Paronal® samples, *i.e. E. coli* L-ASNase preparation without excipients (label claim of 10'000 IU per vial; Kyowa Hakko Kiri Co., Ltd.) (Tokyo, Japan), were obtained from Takeda Pharmaceutical Co., Ltd. (Brussels, Belgium). The polyclonal rabbit antibodies (isotype IgG) against *E. coli* L-ASNase were purchased from Antibody-online GmbH (Aachen, Germany). ERWINASE®, *i.e. Erwinia chrysanthemi* L-ASNase preparation was obtained from EUSA Pharma (Hertfordshire, England). SAW experiments were performed with the five channel SAM®5 Blue from SAW Instruments GmbH (Bonn, Germany; now: NanoTemper Technologies (Munich, Germany)). Unmodified sensor chips (*i.e.* gold layered) were also purchased from SAW Instruments GmbH. PD-10 desalting-column (column I.D. 15 mm, particle size 85–260 µm) was obtained from GE Healthcare (Machelen, Belgium). All SAW experiments were performed at 20 °C using HBS running buffer (10 mM HEPES, pH 7.4 with 150 mM NaCl), with a flow rate of 30 µl/min.

2.2. Preparation of a carboxymethylated dextran hydrogel chip (Supplementary Information 1 for reaction schemes)

The plain gold chips were initially pre-cleaned by a 3 min ultrasonification in deionized water, followed by 3 min in aceton and 3 min in isopropanol. The surface was dried under N_2 stream. A chemical etching proced. was subsequently performed by immersing the chip for 3 min in a freshly prepared boiling solution of 5:1:1 water, ammonia and hydrogen peroxide at 70 °C, to remove all organic residues from the gold layer.

Afterwards, the chip was rinsed in water and dried under N_2 stream [23–25]. Carboxymethylated (CM-) dextran hydrogel chip was prepared following existing proced.s [17]. Briefly, the sensor chip was incubated in a 2 mM 11-mercapto-1-undecanol (MUD) solution in ethanol overnight to form a self-assembled monolayer with end-standing hydroxyl groups. Next, the MUD modified chip was sonicated three times for 2 min in 100% ethanol. Activation of the hydroxyl groups was achieved with 0.6 M epichlorohydrin in a 1:1 mixt. of diglyme and 0.4 M NaOH solution. After the incubation of 4 h, the chip was covered with a 0.3 g/ml dextran in 0.1 M NaOH. Finally the dextran hydrogel was carboxylated by covering the chip in a 1 M bromoacetic acid solution in 2 M NaOH for at least 20 h. The chip was rinsed with water and N_2-dried. The chip was stored at 4 °C in N_2 environment to prevent microbial growth and chemical degradation. The CM-dextran hydrogel chips were used within one month after their preparation.

2.3. Method development (Supplementary Information 2 for reaction schemes)

2.3.1. The immobilization of the pAb

10 µl of 0.1% SDS was first injected to clean up all non-specifically bound molecules on the chip, followed by equilibration with HBS running buffer for 20 min.

2.3.1.1. Immobilization of pAb via amine coupling. The pAb was immobilized according to Ref. [26]: the chip was activated by injection of 130 µl of a 200 mM N-(3-dimethylaminopropyl)-N′-ethylcarbodiimide hydrochloride (EDC) and 50 mM N-hydroxysuccinimide (NHS) mixt. at a flow rate of 12.5 µl/min. Three successive injections of 25 µg/ml pAb in 10 mM sodium acetate buffer pH 4.5 were carried out for 670 s to obtain an effective immobilization of the pAb. Finally, 130 µl of 1 M ethanolamine (pH 8.5) was injected to block the remaining active sites.

2.3.1.2. Immobilization of pAb via thiol coupling. The pAb was first modified with SPDP as follows: an aliquot of 2.5 mM succinimidyl 3-(2-pyridyldithio)propionate (SPDP) in ethanol was added to a solution of 2.5 mg/ml of antibody in 0.1 M phosphate buffer 0.1 M NaCl, pH 7.5, with protein molar ratio of approximately 10 [27]. The mixt. was allowed to react for 1 h at room temperat. and at low agitation. 2.5 ml of above mixt. was transferred to the PD-10 desalting-column; the reaction was stopped by desalting the mixt. using 0.15 M NaCl as the elution buffer. Thiolated antibodies were then prepared by reduction of the SPDP-modified pAb (50 µg/ml) with 50 mM DTT in 50 mM borate buffer, pH 8.5. The mixt. was allowed to react 30 min at room temperat. maintaining a low agitation. The reaction was stopped by PD-10 desalting-column treatment. After activation of the sensor chip with 1:1 EDC:NHS, 20 µl of 80 mM 2-(2-pyridinyldithio) ethaneamine hydrochloride (PDEA, thiol reagent) solution in 0.1 M sodium formate, pH 4.3, were injected. Afterwards, multiple 140 µl injections of the thiolated pAb were performed in order to achieve an efficient immobilization. Finally, 130 µl of 1 M ethanolamine, pH 8.5, was injected to block the remaining active sites. Deactivation of excess reactive disulphides was performed by 20 µl injection of 50 mM L-cysteine in 0.1 M formate buffer containing 1 M NaCl, pH 4.3.

2.3.1.3. EDC-mediated carboxyl coupling. For carboxyl coupling by EDC mediation, the antibody was modified according to the following proced [28]. 6 µM of EDC in 0.1 M 4-morpholinoethanesulfonic acid (MES) buffer pH 4.5 was added to 0.1 mg/ml pAb solution, the mixt. reacts for 2 h in room temperat. The chip was activated by 130 µl 1:1 NHS:EDC injection and modified with hydrazide by 140 µl injection (30 µl/min) of 5 mM carbohydrazide in water. Multiple 140 µl injections of the EDC-modified pAb were performed, then the remaining active esters were inactivated by 130 µl 1 M ethanolamine (pH 8.5) injection. Finally, 0.1 M sodium borohydride in 0.1 M sodium acetate buffer (pH 4.0) was injected for 20 min to stabilize the antibody-modified surface.

2.3.1.4. Immobilization of pAb via aldehyde coupling. For aldehyde immobilization, antibodies were firstly oxidized [27,29]. 2 ml of 50 mM sodium metaperiodate in 0.1 M acetate buffer pH 5.5 was added to 2 ml of 1 mg/ml pAb solution in the same buffer, the mixt. was allowed to react for 20 min in ice. The reaction was stopped by desalting the mixt. on a PD-10 desalting-column with 10 mM sodium acetate buffer (pH 4.0) as the eluent. The chip was activated by 130 µl 1:1 NHS:EDC injection and modified with hydrazide by 140 µl injection of 5 mM carbohydrazide in water. Multiple 140 µl injections of the oxidized-antibody were performed using sodium acetate pH 4.5 as running buffer. Any remaining active esters were inactivated by 130 µl 1 M ethanolamine (pH 8.5) injection. Finally, 0.1 M sodium borohydride in 0.1 M sodium acetate buffer (pH 4.0) was injected for

20 min to stabilize the antibody-modified surface.

2.3.1.5. Immobilization of pAb via protein G. For protein G capturing, 50 µg/ml protein G (in 10 mM sodium acetate buffer pH 4.5) was covalently immobilized to the surface via amine coupling using three 130 µl injections. After deactivation of the remaining active esters by the injection of 130 µl of 1 M ethanolamine (pH 8.5), the pAb was coupled to the protein G by three 140 µl injections of 25 µg/ml pAb in HBS buffer (pH 7.4) [30,31].

2.3.1.6. BS^3 activated amide coupling via protein G. 50 µg/ml protein G (in 10 mM sodium acetate buffer pH 4.5) was covalently immobilized to the surface using amine coupling by performing three 130 µl injections. After the deactivation of the remaining active esters, antibody immobilization was performed by three successive 140 µL injections of 25 µg/ml antibody in acetate buffer, pH 4.5. Then, the 10 µL of 1 mM of the crosslinker bis [sulfosuccinimidyl] suberate (BS^3) was injected by 30 µL/min 100 mM Gly-HCl solution (pH 2.7) was injected, in order to quench the crosslinking reaction and remove unreacted molecules [30,31].

2.3.2. Feasibility evaluation of SAW binding experiments

The signal phase obtained from a SAW biosensor is related to the mass changes caused by the investigated molecules. A prediction of whether a molecule is able to cause a sufficient mass change to obtain a detectable signal is useful to estimate the feasibility of the approach. The following formula is applied to estimate the feasibility of the method. This formula determines the maximum amount of analyte that can be detected, with the assumption that all binding sites of the immobilized pAb are available and active, calculated as follows. A quantitative standard for sensitivity is the equipment specific detection limit of 0.5 pg/mm^2 [32], indicated as follows:

$$X = \frac{P \times MW_A \times f}{S \times MW_L} > 0.5 \frac{pg}{mm^2}$$

where, X: the theoretical area-concentration of bound analyte (in pg/mm^2); P: the phase shift (°) related to surface immobilized pAb; MW_A is the molecular weight of the analyte (in 136 320 pg/pmol); MW_L is the molecular weight of the pAb (in 150 000 pg/pmol); S: the conversion factor and is equipment specific (*i.e.* 0.0515°mm^2/pg); f: binding stoichiometry, in the case of pAb, f was taken 2.

2.3.3. Relative response

The different immobilization techniques were compared using normalized response values, calculated as follows:

$$RR_{\%} = \varphi_{analyte} / \varphi_{max} \times 100$$

where, RR% = the relative response (%); $\varphi_{analyte}$ = phase shift (°) of analyte injection at 350s (the equilibrium state at association phase) and φ_{max} = maximum phase shift upon *E. coli* L-ASNase binding (°) *i.e.* phase shift if all immobilized pAb are occupied, calculated with the formula $\varphi_{max} = X \times S$, where X is the theoretical area-concentration of bound analyte (in pg/mm^2) and S: the conversion factor and is equipment specific (*i.e.* 0.0515°mm^2/pg).

2.3.4. Percentage non-specific binding

Non-specific binding was expressed as the ratio of the BSA response to the L-ASNase response:

$$NSB_{\%} = \varphi_{BSA} / \varphi_{analyte} \times 100$$

where, NSB% = the relative amount of non-specific binding (%); φ_{BSA} = phase shift of 100 nM BSA injection at 350s (°) and $\varphi_{analyte}$ = phase shift of 100 nM L-ASNase injection at 350s (°).

2.3.5. Binding behavior

The binding behaviour was studied using 0, 10, 25, 50, 100, 150, 200, 250, 300, 350 and 400 nM E. *coli* L-ASNase in HBS (20 mM HEPES, 150 mM NaCl, pH 7).

2.4. Final method

Prior to the assay experiment, a carboxymethylated dextran hydrogel chip was prepared according to the proced. in Section 2.2. The pAb was immobilized on the chip as following: 50 µg/ml protein G (in 10 mM sodium acetate buffer pH 4.5) was covalently immobilized to the surface using amine coupling by performing three 130 µl injections. Further on, three successive 140 µL of 25 µg/ml antibody was injected in acetate buffer, pH 4.5. Then, the 10 µL of 1 mM of the BS^3 was injected by 30 µL/min. Finally, 100 mM Gly-HCl solution (pH 2.7) was injected.

The assay experiment was performed at 30 µl/min over the SAW chip using HBS (20 mM HEPES, 150 mM NaCl, pH 7.4) as running buffer. 200 µl of reference solution or sample solution was injected (400 s duration), followed by a 10 min dissociation phase, during which only HBS buffer was passed over the surface. After the dissociation, regeneration was carried out with 30 µl regeneration solution consisting of 25 mM NaOH and 0.05% SDS, followed by two 30 µl HBS buffer injections to prevent carry-over. In addition, a blank injection (HBS running buffer) was performed prior to each binding experiments and its response was subtracted from the response of the analyte injections. 5, 8, 10, 12 and 15 nM L-ASNase solutions in HBS buffer (20 mM HEPES, 150 mM NaCl, pH 7.4) were injected as the reference solutions for the fitting of calibration curve. 10 nM sample solution (*i.e.* 0.136 µg/ml L-ASNase as commercially available) in HBS buffer was injected for the assay, corresponding to the theoretical 100% label claim (l.c.). The response (y) is the phase (°) at 350 s, *i.e.* at the equilibrium steady state of association stage.

2.5. Method validation

For the selectivity test, *E. coli* L-ASNase was compared with *Erwinia chrysanthemi* L-ASNase (ERWINASE®), injecting 50 and 200 nM of each. For the validation of the calibration curve, 5, 8, 10, 12 and 15 nM L-ASNase solution was injected as the reference solutions (n = 15). The response (y) is the phase (°) at 350 s, *i.e.* at the equilibrium steady state of association stage. The recovery is calculated as the ratio between the concentration found and the theoretical concentration.

3. Results and discussion

3.1. Method development

3.1.1. Selection of immobilization method

Different immobilization proced.s have been described for proteins and antibodies, which can be classified in two main groups: random immobilization (*i.e.* amine coupling, sulfhydryl coupling, hydrazide -activated carbonyl coupling, and EDC-mediated carboxyl coupling) and site-directed immobilization (*i.e.* protein G coupling, and BS^3 activated amide coupling via protein G) [33]. Since the immobilization does not always result in active pAb, the binding sites can be inactive or inaccessible, the choice of immobilization strategies play a significant role for the signal magnitude [34]. Therefore, four responses have been applied to select the most suitable immobilization method: surface immobilized pAb density, absolute response, normalized response and percentage non-specific binding (Fig. 1). First, the surface immobilized pAb density was investigated: the concentration of total bound L-ASNase of each immobilization strategy exceeded the theoretical limit of detection of 0.5 pg/mm^2 (Fig. 1A), indicating a detectable *E. coli* L-ASNase signal by each immobilization strategy [32]. The immobilization of L-ASNase using amine coupling resulted in the highest active

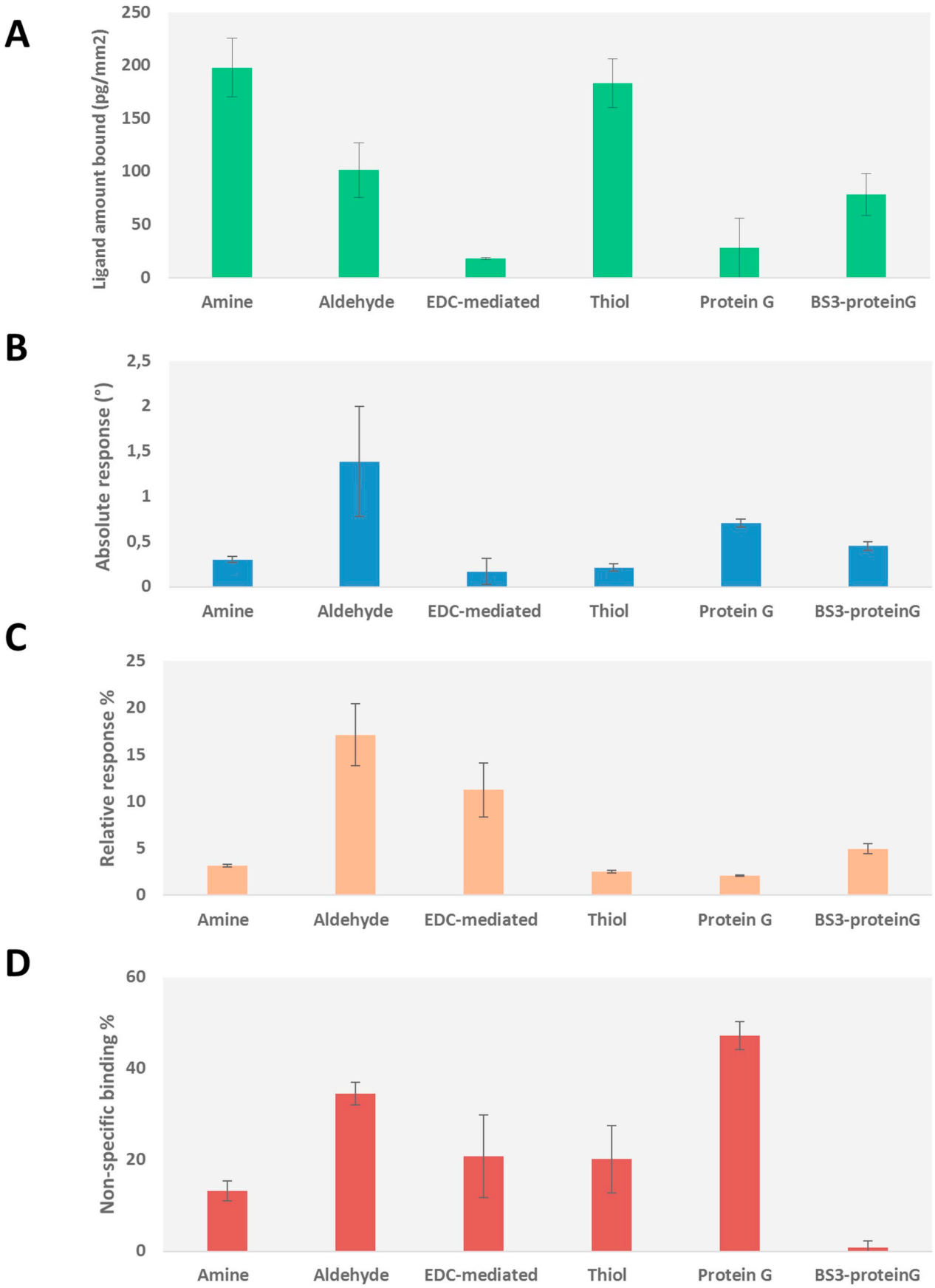

Fig. 1. Quantitative evaluation of immobilization strategies. A. Surface immobilized pAb density (pg/mm^2). B. Absolute response of L-ASNase (phase, °). C. Normalized response values (RR %). D. Percentage non-specific binding (NSB %). Mean values are represented, with the error bars representing the standard deviation (amine n = 4; aldehyde n = 2; EDC-mediated n = 4; thiol n = 5; protein G n = 5; BS^3-protein G n = 5).

pAb surface (187.7 ± 27.5 pg/mm^2, Supplementary Information 3), while the density of immobilized pAb by EDC-mediated coupling is the lowest (17.0 ± 1.1 pg/mm^2). Secondly, the absolute response being the phase value after the injection of L-ASNase showed the highest value for the aldehyde immobilization (Fig. 1B). Moreover, the relative response RR% is a normalised value of the determined phase (at 350 s) of *E. coli* L-ASNase solution relative to the theoretical maximum phase shift (at 350 s) upon *E. coli* L-ASNase binding (see Section 2.3.3). RR% was applied to compare the binding capability (*i.e.* the remaining activity of the pAb binding sites on the chip surface) between different immobilization methods. The random orientation of the pAb often results in loss of the binding capability of analyte, with for the amine coupling a RR% value of 3.1 ± 0.1% was obtained (Fig. 1C) [35]. The RR% for the protein G coupling immobilization is quite low (RR % = 2.0 ± 0.1%), which can also be due to dissociation of the pAb-protein G complex after immobilization. Finally, the selectivity was quantitatively expressed as NSB% using a negative control BSA. The NSB% expresses the ratio of the signal of a "random" protein (*e.g.* BSA) related to an analyte signal. The "random" protein is associated with the dextran layer and gold via non-selective interactions. The NSB% is preferably as low as possible. The linker BS^3 fixes the pAb on the protein G, therefore this immobilization is expected to have the highest selectivity, which was confirmed by its low NSB% (0.9 ± 0.3%, Fig. 1D). Overall, BS^3 activated amide coupling via protein G had a relatively high RR% and a low NSB%; therefore, this approach was taken as the final immobilization method.

3.1.2. Binding behaviour

According to the binding model $\frac{[L][A]}{[LA]} = \frac{k_{off}}{k_{on}} = K_d$, the complex *[LA]* can be calculated as $[LA] = \frac{[L_T][A]}{K_d + [A]}$ (Equation 1), which is a rational function. *[L], [A] and [LA]* represent the concentrations of "free" ligand and analyte, and the concentration of complex respectively. The k_{on}, k_{off} and K_d are respectively the on-rate constant, off-rate constant and equilibrium dissociation constant, where the total concentration $[L_T]$ equals to $[L] + [LA]$ [36]. When the free concentration of analyte [A] is low, Equation 1 equals to $[LA] = \frac{[L_T]}{K_d}[A]$ with a slope of $\frac{[L_T]}{K_d}$. With increasing [A] concentration, the binding active sites of the immobilized ligand will become fully occupied with the analytes, and the association state gets to equilibrium state ($[LA] = [L_T]$). The rate of uptake of the analytes equals to the rate of release of the analyte from the complex, which is observed after 350 s (Fig. 2A). The response (phase in °) at 350 s (equilibrium state) increases steeply in the concentration range of 0–25 nM of L-ASNase, with plateauing beyond 50 nM (Fig. 2B). The binding active sites on the surface are then fully occupied and the slight steady increase in phase is thus caused by mass transport limitation [37,38]. This binding behavior was important for the calibration curve in the assay, which was thus focused in the 5–15 mM range.

3.2. Method validation

The sensorgram of *E. coli* L-ASNase showed a kinetic association, followed by a dissociation step, while *Erwinia* L-ASNase showed no interaction (Fig. 3), indicating that the developed SAW biosensor method is selective for the *E. coli* L-ASNase.

The calibration curve for the functional quantification of L-ASNase was investigated using the concentration range of 5–15 nM, *e.g.* 5, 8, 10 (*i.e.* 100% l.c.), 12 and 15 nM. A quadratic model was found to be the best fit for the quantification of *E. coli* L-ASNase, yielding the equation $y = -0.0008x^2 + 0.0249x - 0.0091$, with an ANOVA F value of 242 and R^2 of 0.9959 (Fig. 4). The 95% confidence interval (95% CI) of the coefficients were 0.0014 to −0.0003 for −0.0008, 0.0138 to 0.036 for 0.0249, and −0.061 to 0.0428 for −0.0091 (hence, including the zero). The recovery is calculated as the ratio between the concentration found and the theoretical concentration. The precision is calculated as the relative standard deviation (RSD%) of the equilibrium phase of each meas. ments. The recovery is 102.4%, with the precision of 8.5% for 10 nM (n = 15).

3.3. Application

The applicability of the developed and validated method was demonstrated by analyzing several L-ASNase samples: a commercial batch of *E. coli* L-ASNase, another *E. coli* L-ASNase batch from the same supplier, a stress-degraded dry-heated (80 °C, 10 min) *E. coli* L-ASNase and a deamidated *E. coli* L-ASNase. The results obtained were 101.0% l.c. (RSD of 6.5%) and 100.7% l.c. (RSD of 13.7%) for both batches of *E. coli* L-ASNase of the same supplier, confirming the quality consistence as expected from pharmaceutical GMP. The stress-degraded sample, obtained by a short period of dry heating, showed a reduced assay value of 93.8% l.c. (RSD of 5.7%). The deamidated *E. coli* L-ASNase showed an assay value of 90.3% l.c. (RSD of 8.3%), also well below the generally accepted specification limit of 95% l.c.

4. Conclusion

A SAW method for the functional quantification of *E. coli* L-ASNase was developed. Several immobilization strategies were first quantitatively evaluated by the immobilized pAb density, absolute response, normalized response and non-specific binding, leading to the BS^3 activated amide coupling via protein G strategy as final immobilization method. After the binding behavior was characterized, a final method was proposed, which was validated. Finally, this validated method was

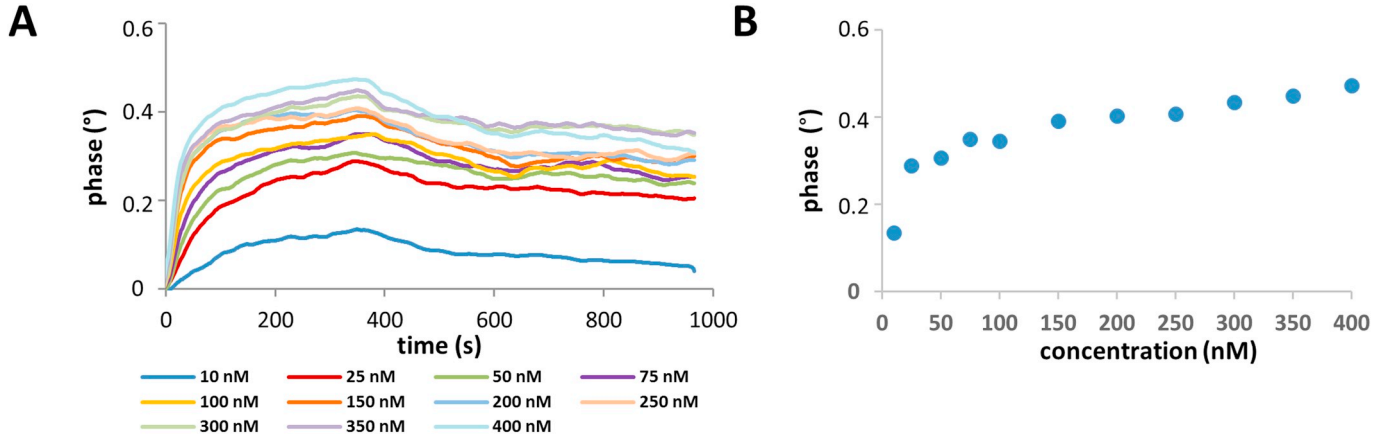

Fig. 2. A: SAW sensorgrams of L-ASNase and pAb interaction (L-ASNase concentration of 0–400 nM). B: Phase (°) responses at 350 s (equilibrium state) with different L-ASNase concentrations in the range of 0–400 nM.

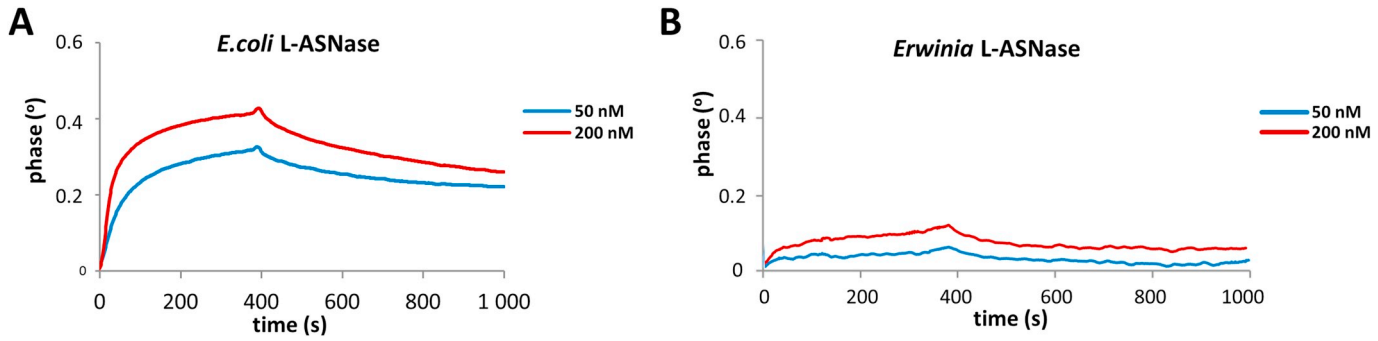

Fig. 3. SAW sensorgrams of L-ASNase and pAb interaction. A. 50 and 200 nM of *E. coli* L-ASNase. B. 50 and 200 nM of *Erwinia* L-ASNase.

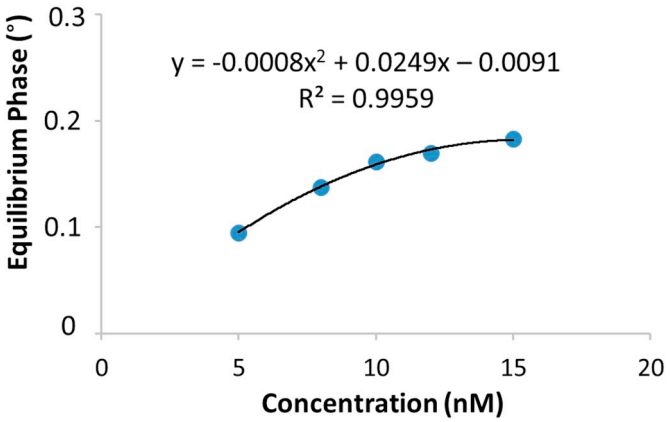

Fig. 4. Quadratic regression, visualizing the phase (°) at equilibrium (*i.e.* at 350 s) in function of L-ASNase concentration of 5, 8, 10 (*i.e.* 100% l. c.), 12 and 15 nM.

applied on different *E. coli* L-ASNase samples. This developed SAW method can thus be adopted as a pharmaceutical quality control method for L-ASNase medicines and proves the usefulness of biosensors in QC of biologics.

Acknowledgements

The authors would like to thank the Ph.D. grant of the China Scholarship Council (CSC) to Han Yao (201206220137) and Xiaolong Xu (201406160087). Takeda Pharmaceutical Co., Ltd. (Brussels, Belgium) is acknowledged for supplying *E. coli* L-asparaginase preparation (Paronal®).

Appendix A. Supplementary data

Supplementary data to this article can be found online at https://doi.org/10.1016/j.talanta.2019.05.046.

References

[1] C.H. Pui, L.L. Robison, A.T. Look, Acute lymphoblastic leukaemia, Lancet (London, England) 371 (2008) 1030–1043.
[2] A.L. Swain, M. Jaskolski, D. Housset, J.K. Rao, A. Wlodawer, Crystal struct. of Escherichia coli L-asparaginase, an enzyme used in cancer therapy, Proc. Natl. Acad. Sci. U.S.A. 90 (1993) 1474–1478.
[3] J.C. Wriston Jr., Asparaginase, Methods Enzymol. 113 (1985) 608–618.
[4] K.B. McCredie, D.H.W. Ho, E.J. Freireich, L-asparaginase for the treatment of cancer, CA A Cancer J. Clin. 23 (1973) 220–227.
[5] K. Kumar, J. Kaur, S. Walia, T. Pathak, D. Aggarwal, L-asparaginase: an effective agent in the treatment of acute lymphoblastic leukemia, Leuk. Lymphoma 55 (2014) 256–262.
[6] E.A. Raetz, W.L. Salzer, Tolerability and efficacy of L-asparaginase therapy in pediatric patients with acute lymphoblastic leukemia, J. Pediatr. Hematol. Oncol. 32 (2010) 554–563.
[7] K.K. Kanazawa, J.G. Gordon, Frequency of a quartz microbalance in contact with liquid, Anal. Chem. 57 (1985) 1770–1771.
[8] M.I. Rocha-Gaso, C. March-Iborra, A. Montoya-Baides, A. Arnau-Vives, Surface generated acoustic wave biosensors for the detection of pathogens: a review, Sensors (Basel) 9 (2009) 5740–5769.
[9] T.M. Gronewold, Surface acoustic wave sensors in the bioanalytical field: recent trends and challenges, Anal. Chim. Acta 603 (2007) 119–128.
[10] N. Barie, M. Rapp, Covalent bound sensing layers on surface acoustic wave (SAW) biosensors, Biosens. Bioelectron. 16 (2001) 979–987.
[11] P. Verma, R.D.S. Yadava, Polymer selection for SAW sensor array based electronic noses by fuzzy c-means clustering of partition coefficients: model studies on detection of freshness and spoilage of milk and fish, Sensor. Actuator. B Chem. 209 (2015) 751–769.
[12] O. Onen, A. Sisman, N.D. Gallant, P. Kruk, R. Guldiken, A urinary Bcl-2 surface acoustic wave biosensor for early ovarian cancer detection, Sensors (Basel) 12 (2012) 7423–7437.
[13] A. Tretjakov, V. Syritski, J. Reut, R. Boroznjak, A. Opik, Molecularly imprinted polymer film interfaced with Surface Acoustic Wave technology as a sensing platform for label-free protein detection, Anal. Chim. Acta 902 (2016) 182–188.
[14] X. Liu, J.Y. Wang, X.B. Mao, Y. Ning, G.J. Zhang, Single-shot analytical assay based on graphene-oxide-modified surface acoustic wave biosensor for detection of single-nucleotide polymorphisms, Anal. Chem. 87 (2015) 9352–9359.
[15] K. Chang, Y. Pi, W. Lu, F. Wang, F. Pan, F. Li, S. Jia, J. Shi, S. Deng, M. Chen, Label-free and high-sensitive detection of human breast cancer cells by aptamer-based leaky surface acoustic wave biosensor array, Biosens. Bioelectron. 60 (2014) 318–324.
[16] Y.W. Kim, M.T. Meyer, A. Berkovich, S. Subramanian, A.A. Iliadis, W.E. Bentley, R. Ghodssi, A surface acoustic wave biofilm sensor integrated with a treatment method based on the bioelectric effect, Sens. Actuator Phys. 238 (2016) 140–149.
[17] N. Bracke, S. Barhdadi, E. Wynendaele, B. Gevaert, M. D'Hondt, B. De Spiegeleer, Surface acoustic wave biosensor as a functional quality method in pharmaceutics, Sensor. Actuator. B Chem. 210 (2015) 103–112.
[18] M. Csete, W.D. Hunt, Potential of surface acoustic wave biosensors for early sepsis diagnosis, J. Clin. Monit. Comput. 27 (2013) 427–431.
[19] K. Chang, F. Wang, Y. Ding, F. Pan, F. Li, S. Jia, W. Lu, S. Deng, J. Shi, M. Chen, Development and validation of a novel leaky surface acoustic wave immunosensor array for label-free and high-sensitive detection of cyclosporin A in whole-blood samples, Biosens. Bioelectron. 54 (2014) 151–157.
[20] V.I. Avramis, E.V. Avramis, W. Hunter, M.C. Long, Immunogenicity of native or pegylated E. coli and Erwinia asparaginases assessed by ELISA and surface plasmon resonance (SPR-biacore) assays of IgG antibodies (Ab) in sera from patients with acute lymphoblastic leukemia (ALL), Anticancer Res. 29 (2009) 299–302.
[21] A. Aubé, D.M. Charbonneau, J.N. Pelletier, J.-F. Masson, Response monitoring of acute lymphoblastic leukemia patients undergoing l-asparaginase therapy: successes and challenges associated with clinical sample analysis in plasmonic sensing, ACS Sens. 1 (11) (2016) 1358–1365.
[22] N.E. Labrou, M.M. Muharram, Biochemical characterization and immobilization of Erwinia carotovoral-asparaginase in a microplate for high-throughput biosensing of l-asparagine, Enzym. Microb. Technol. 92 (2016) 86–93.
[23] L.M. Fischer, M. Tenje, A.R. Heiskanen, N. Masuda, J. Castillo, A. Bentien, J. Émneus, M.H. Jakobsen, A. Boisen, Gold cleaning methods for electrochemical detection applications, Microelectron. Eng. 86 (2009) 1282–1285.
[24] S.K. Vashist, A method for regenerating gold surface for prolonged reuse of gold-coated surface plasmon resonance chip, Anal. Biochem. 423 (2012) 23–25.
[25] D.J. Kim, R. Pitchimani, D.E. Snow, L.J. Hope-Weeks, Hope-Weeks, A simple method for the removal of thiols on gold surfaces using an NH4OH-H2O2-H2O solution, Scanning 30 (2008) 118–122.
[26] B. Johnsson, S. Lofas, G. Lindquist, Immobilization of proteins to a carboxymethyldextran-modified gold surface for biospecific interaction analysis in surface plasmon resonance sensors, Anal. Biochem. 198 (1991) 268–277.
[27] S. Löfås, B. Johnsson, Å. Edström, A. Hansson, G. Lindquist, R.-M.M. Hillgren, L. Stigh, Methods for site controlled coupling to carboxymethyldextran surfaces in surface plasmon resonance sensors, Biosens. Bioelectron. 10 (1995) 813–822.
[28] P. Kocbek, N. Obermajer, M. Cegnar, J. Kos, J. Kristl, Targeting cancer cells using PLGA nanoparticles surface modified with monoclonal antibody, J. Control. Release 120 (2007) 18–26.
[29] M.J. Fischer, Amine coupling through EDC/NHS: a practical approach, Methods Mol. Biol. 627 (2010) 55–73.

[30] M. Soler, M.C. Estevez, M. Alvarez, M.A. Otte, B. Sepulveda, L.M. Lechuga, Direct detection of protein biomarkers in human fluids using site-specific antibody immobilization strategies, Sensors 14 (2014) 2239–2258.
[31] H.Y. Song, X. Zhou, J. Hobley, X. Su, Comparative study of random and oriented antibody immobilization as meas.d by dual polarization interferometry and surface plasmon resonance spectroscopy, Langmuir 28 (2012) 997–1004.
[32] M.D. Schlensog, T.M.A. Gronewold, M. Tewes, M. Famulok, E. Quandt, A Love-wave biosensor using nucleic acids as ligands, Sensor. Actuator. B Chem. 101 (2004) 308–315.
[33] B.J. Sutton, D.C. Phillips, The three-dimensional struct. of the carbohydrate within the Fc fragment of immunoglobulin G, Biochem. Soc. Trans. 11 (1983) 130–132.
[34] S.K. Vashist, C.K. Dixit, B.D. MacCraith, R. O'Kennedy, Effect of antibody immobilization strategies on the analytical performance of a surface plasmon resonance-based immunoassay, Analyst 136 (2011) 4431–4436.
[35] D.J. O'Shannessy, M. Brigham-Burke, K. Peck, Immobilization chemistries suitable for use in the BIAcore surface plasmon resonance detector, Anal. Biochem. 205 (1992) 132–136.
[36] E.C. Hulme, M.A. Trevethick, Ligand binding assays at equilibrium: validation and interpretation, Br. J. Pharmacol. 161 (2010) 1219–1237.
[37] D.B. Hibbert, J.J. Gooding, P. Erokhin, Kinetics of irreversible adsorption with Diffusion: application to biomolecule immobilization, Langmuir 18 (2002) 1770–1776.
[38] P. Schuck, H. Zhao, The role of mass transport limitation and surface heterogeneity in the biophysical characterization of macromolecular binding processes by SPR biosensing, Methods Mol. Biol. 627 (2010) 15–54.